

Extended Essay: Physics

Title: The Relationship Between Polygon Geometry and Vortex Shedding Frequency in a Two-Dimensional Laminar Flow

RQ: How does increasing the number of faces of a bluff body (ranging from 2 to 12) affect the vortex shedding frequency in laminar flow, measured in Hz, in a two-dimensional plane?

Word count:

...

Contents

| | | |
|----------|--|-----------|
| 1 | Introduction | 2 |
| 2 | Background | 3 |
| 2.1 | Frequency and Time Period | 3 |
| 2.2 | Fundamentals of Fluid Dynamics | 3 |
| 2.3 | Vortex Shedding and the Kármán Vortex Street | 4 |
| 2.4 | The Mechanism of Vortex Shedding | 4 |
| 2.5 | The Bluff Body | 7 |
| 2.6 | Hypothesis | 7 |
| 3 | The Two Investigations | 8 |
| 3.1 | The Theoretical Investigation | 8 |
| 3.1.1 | Ansys Workbench | 8 |
| 3.1.2 | The OpenFoam Simulation | 9 |
| 3.1.3 | Simulation Settings | 9 |
| 3.2 | The Practical Investigation | 12 |
| 3.3 | Determining the vortex shedding frequency | 16 |
| 4 | Variables | 17 |
| 5 | Equipment | 18 |
| 6 | Method | 19 |

1 Introduction

Despite its widespread significance, the study of fluid dynamics is largely overlooked by the IB Physics syllabus. Defined as a field of applied science dedicated to studying the motion and interaction of fluid substances, fluid dynamics is one of the two sub-fields of fluid mechanics, the field concerned with understanding the dynamics of fluids subject to external forces (Ghose, 2014).

From the air we breathe to the water we consume; fluids are present in almost every aspect of our lives. Although observing fluids in action is a daily occurrence for all, countless remain unaware of the highly complex and intricate theories governing these seemingly simple and elementary phenomena. Ultimately, a profound youthful interest in cars and planes — everything with an engine really — coupled with a fascination for the motion of fluids led to the topic of this essay: vortex shedding. Specifically, this essay will concern itself with the question: *How does increasing the number of faces of a bluff body (ranging from 2 to 12) affect the vortex shedding frequency in laminar flow, measured in Hz, in a 2D plane?*

Over the past century, vortex shedding has garnered a multifold of attention, with hundreds of papers published (Buresti, 1998, p. 61). This partially elucidated phenomenon is quintessential in a broad range of scientific and engineering contexts, from maintaining ubiquitous infrastructure to developing cutting-edge aerospace technologies. Bridges may suffer from vortex shedding excitation, a severe challenge which undermines their structural integrity (Jurado et al., 2012, p. 1040). This was exemplified by the collapse of the Tacoma Narrows Bridge on the 7th of November 1940, where vortex shedding acted as the instigating mechanism – triggering vertical vibration that eventually transitioned into the torsional oscillations, ultimately causing its collapse (Song et al., 2022).

As previously mentioned, the IB Physics Guide (“IB Physics Guide 2025”, 2023) does not directly concern itself with vortex shedding or, in general, the majority of fluid dynamics. Nevertheless, links can be made to section C: “Wave Behavior”. Section C.1, “Simple Harmonic Motion”, concerns itself with, as the name suggests, simple harmonic motion, an idealized theoretical representation of the behavior of oscillatory systems (Allum & Morris, 2023, p. 313). Fundamental concepts such as frequency and time period are discussed, ideas required in order to analyze the frequency of the vortex shedding caused by a bluff body. Furthermore, the topic of this essay also links to section C.4, “Standing Waves and Resonance”. Concepts of natural frequency, vibrations and resonance are key when discussing the problems caused by vortex shedding, like the one detailed above, and the significance of the frequency of vortex shedding.

2 Background

2.1 Frequency and Time Period

Frequency is defined as the number of occurrences of a periodic event per unit time (Allum & Morris, 2023, p. 78). **Time period** is referred to as the amount of time between each iteration of an event which happens periodically (Allum & Morris, 2023, p. 78). These two terms stand in an inverse relationship

$$f = \frac{1}{T} \quad (1)$$

where f is frequency in Hz and T is time period in seconds. This relationship is later utilized to extrapolate the vortex shedding frequency in both the theoretical and the practical investigation.

2.2 Fundamentals of Fluid Dynamics

The definition of vorticity, a vortex and a bluff body must be understood. **Vorticity** is the vector quantity representing the rotational motion in a velocity field (Holton, 2003, p. 2500). A **vortex** is the circular flow of a fluid around a central axis, characterized by the vorticity in the fluid (Nitsche, 2006, p. 390). A **bluff body** is defined as an object that, due to its geometry, induces significant regions of separated flow (National Research Council, 1997, p. 561).

Furthermore, one must distinguish between a Newtonian and a non-Newtonian fluid. A **Newtonian fluid** is a fluid in which the viscosity — a measure of internal friction — remains constant despite applied shear rate, whereas a **non-Newtonian** fluid exhibits a viscosity which varies with the applied force (Mohn, 2024).

Moreover, one must also consider the type of flow. There are two key factors of flow when investigating vortex shedding: laminar and turbulent flow, and compressible and incompressible flow. **Laminar flow** is characterized by the layered motion of fluid particles, with no significant disturbance between the parallel layers (Versteeg & Malalasekera, 2007, pp. 40–41). On the other hand, **turbulent flow** is known to have continuous, irregular fluctuations in velocity and pressure throughout the fluid (Versteeg & Malalasekera, 2007, p. 40). A **compressible flow** is a flow in which the fluid does not have a uniform density (Oran & Boris, 2002, p. 31), conversely, an **incompressible flow** is a flow in which the fluid has a constant density (Versteeg & Malalasekera, 2007, p. 12).

Lastly, two dimensionless numbers must be considered: the Reynolds and Strouhal number. The **Reynolds number** expresses the “ratio between inertial and viscous forces” (NASA Glenn Research Center, 2021; “The Relationship Between Reynolds Number and Kinematic Viscosity”, n.d.). Given by the equation

$$Re = \frac{UL}{\nu} \quad (2)$$

where U is the free-stream velocity ($m\ s^{-1}$), L is the characteristic length (m) and ν is the kinematic viscosity ($m^2\ s^{-1}$). This number allows one to classify if a flow is laminar or turbulent, with low Reynolds numbers signifying laminar flow and high Reynolds number indicating turbulent flow (Saldana et al., 2024). The **Strouhal number** is a dimensionless parameter used to describe the periodicity of vortex shedding (Choi & Kwon, 2000, p. 211). It is given by the equation

$$St = \frac{fL}{U} \quad (3)$$

where f is the frequency of vortex shedding (Hz), L is the characteristic length (m) and U is the free-stream velocity ($m\ s^{-1}$). A high Strouhal number — assuming both L and U remain constant — indicates an increased vortex shedding frequency f , conversely a low Strouhal number indicates a lower f .

This essay will analyze vortex shedding in a Newtonian fluid — water — which exhibits laminar and incompressible flow. A Reynolds number of 100 was targeted in order to ensure laminar flow (Alammar, n.d. p. 2); however, due to practical limitations, this was only fully realized theoretically and not in practice — details of which are discussed later.

2.3 Vortex Shedding and the Kármán Vortex Street

Vortex shedding in a two-dimensional plane can be defined as the phenomenon in which localized regions of high vorticity are periodically released into the wake from alternating sides of a bluff body, each exhibiting an opposite rotational direction (Green, 1995, p. 156). Whereas vortex shedding is the process by which vortices are formed, Kármán Vortex Street refers to the flow pattern created, a repeated structure of counter-rotating vortices (Govardhan & Ramesh, 2005, p. 26).



Figure 1: Von Kármán Street behind a cylinder in a non-rotating 2D flow for $Re = 140$, fluorescein visualization (Ilieva, 2017, p. 144)

2.4 The Mechanism of Vortex Shedding

Due to the friction between a given fluid and a bluff body, there is no relative motion between them (Jeff Defoe, 2020; TutorialsPoint, 2018). Consequently, if the velocity of the bluff body is zero, the velocity of the fluid at the wall of the bluff body, with respect to the reference frame of the bluff body, is also zero: a no-slip condition. This causes a variation in velocities with distance, from zero at the bluff body surface to the free stream velocity U at a certain distance from the bluff body. The region in which this velocity gradient occurs is referred to as the boundary layer.

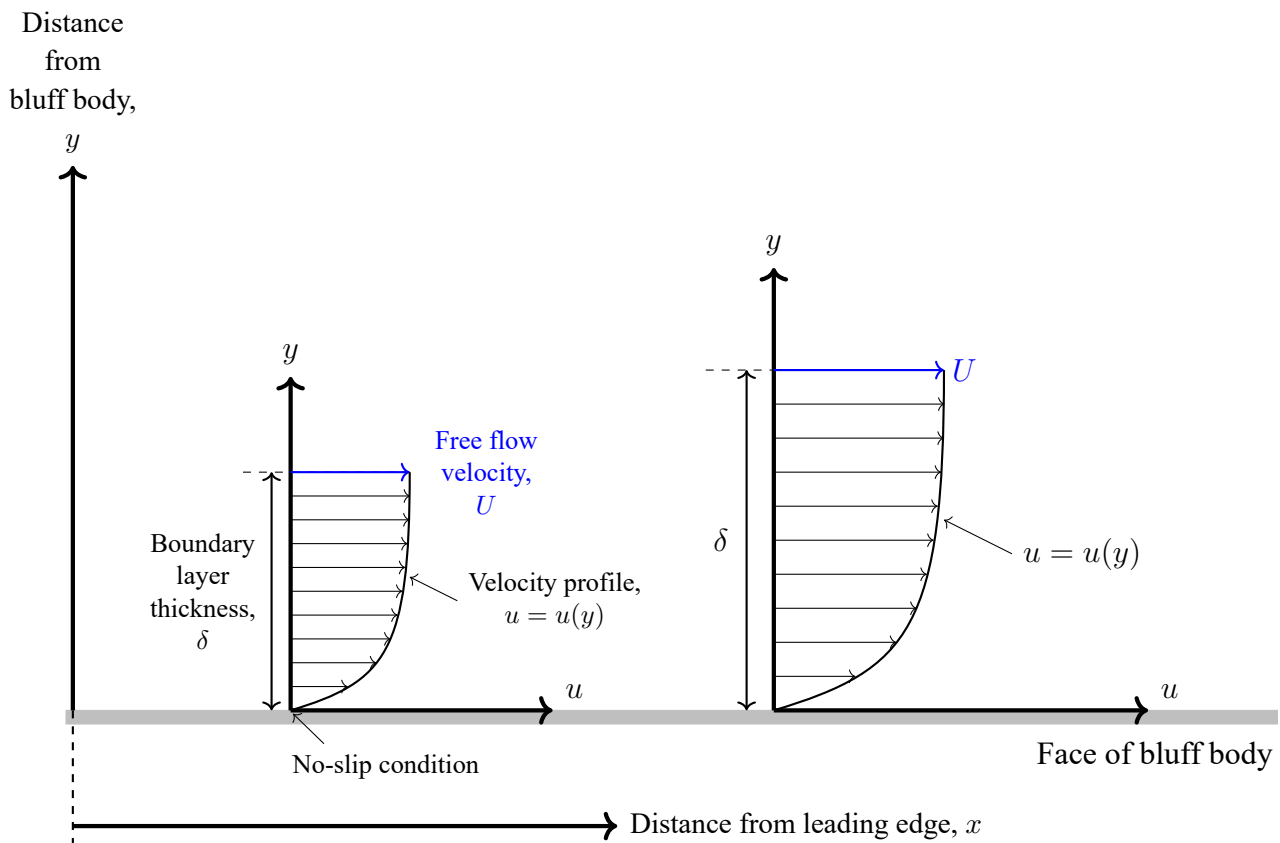


Figure 2: Depiction of boundary layer and the velocity gradient formed. Inspired by Embry-Riddle Aeronautical University (n.d.)

When a flow moves past a bluff body in a two-dimensional plane, a boundary layer develops, with increasing thickness δ from the stagnation point (Fitzpatrick, 2016), the point on the leading edge of the bluff body at which the local fluid velocity is zero (with respect to the bluff body), to the back of the bluff body (Learn Engineering, 2022). At a certain point, the boundary layer separates from the bluff body, forming a shear layer. Under steady flow conditions, this separation occurs in a periodic and alternating manner, creating two separate, out-of-phase shear layers on either side of the bluff body.

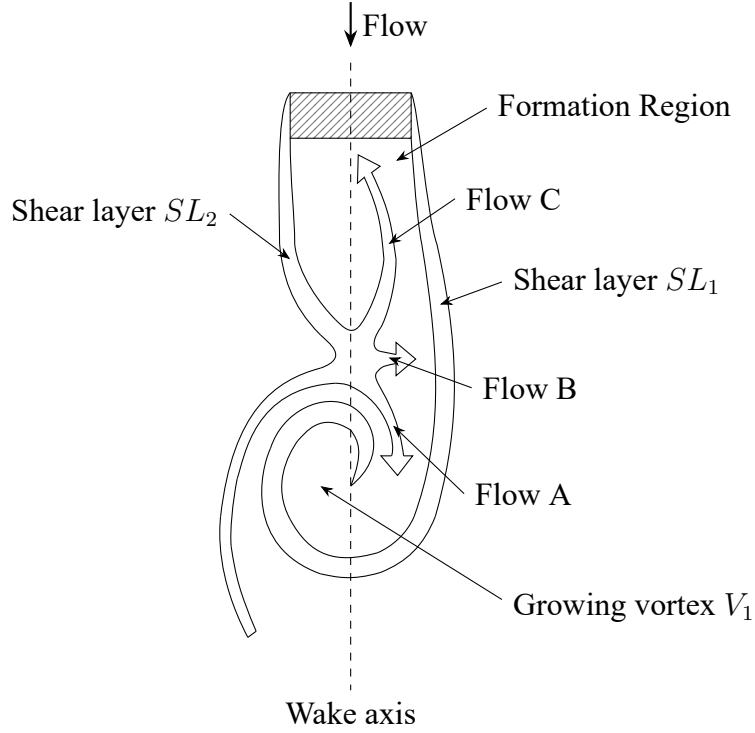


Figure 3: The mechanism of vortex shedding. Inspired by Shen et al. (2010, p. 3)

For simplification, assume the first shear layer is generated at the right of the bluff body (SL_1). Due to its vorticity, the shear layer tends to curl up, forming a vortex. As the vortex forms, the pressure in the core of the vortex decreases, acting as a sink, inducing inflow towards its center. The fluid initially present at the bottom of the backside of the bluff body is drawn into the vortex, creating space, allowing for the formation of the left shear layer (SL_2) in the *formation region*. This newly created shear layer splits into three distinct flows: a flow (*Flow C*) which recirculates behind the bluff body, a flow (*Flow B*) which mixes with the top shear layer and a flow (*Flow A*) which is drawn into the vortex (V_1).

There is a decrease in strength of the vortex being created due to *Flow A* having an opposite vorticity to the vorticity of the vortex. Moreover, the opposite vorticity of *Flow B* and the right shear layer effectively nullifies each other, leading to the right shear layer being interrupted and the vortex becoming detached, causing it to travel with the main flow. The vortex has been “shed”. Since the vortex moves away from the bluff body, its low-pressure influence on the area near the bluff body decreases, allowing the left shear layer to more freely develop. Now, due to the periodic nature of vortex formation, the process recurs with the shear layers switching roles.

When considering the vortex being created from the top shear layer, the fluid at the top of the vortex will have the same velocity as the free stream velocity U , whereas the velocity at the bottom of the vortex will be of a smaller magnitude and in the opposite direction of the main flow. According to Bernoulli’s equation, a region of higher velocity must have a lower pressure and vice versa. Therefore, the bottom region of the vortex will have a higher pressure than the top region, causing a lift force which acts on the bluff body normal to the flow. The oscillation of this lift force coincides with the vortex shedding frequency f , the frequency at which the vortices are alternately shed from opposite sides of the bluff body.

2.5 The Bluff Body

In order to maintain a cylinder-like appearance, one of the most common bluff bodies investigated (Rocchi & Zasso, 2002, p. 475), this investigation is conducted with bluff bodies which have a rectangular “tail”, in order to give each shape an equal overall length ℓ in both streamwise and transverse directions. The bluff body faces facing the inlet are of the same length.

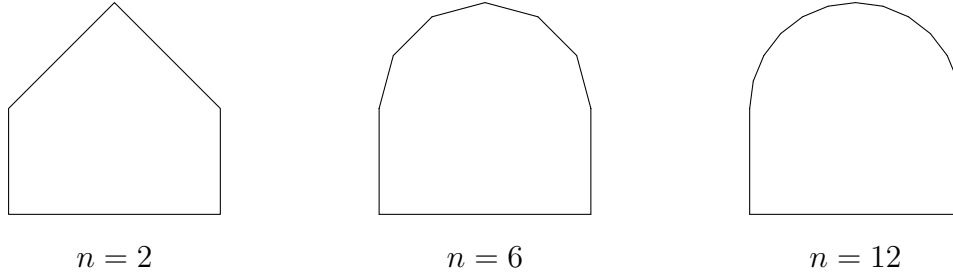


Figure 4: Examples of bluff bodies

2.6 Hypothesis

It is hypothesized that as the number of faces of the bluff body increases from 2 to 12, the vortex shedding frequency in laminar flow will decrease. This trend is attributed to a decrease in the Strouhal number (Gonçalves & Del Rio Vieira, 1999) which is directly proportional to the vortex shedding frequency, as seen in Equation (3)

3 The Two Investigations

3.1 The Theoretical Investigation

3.1.1 Ansys Workbench

The geometry and mesh preparation for the simulation was conducted using Ansys Workbench (“Ansys Workbench | Simulation Integration Platform”, n.d.). The dimensions of the fluid domain are based on 5 where ℓ is the overall length of the bluff body.

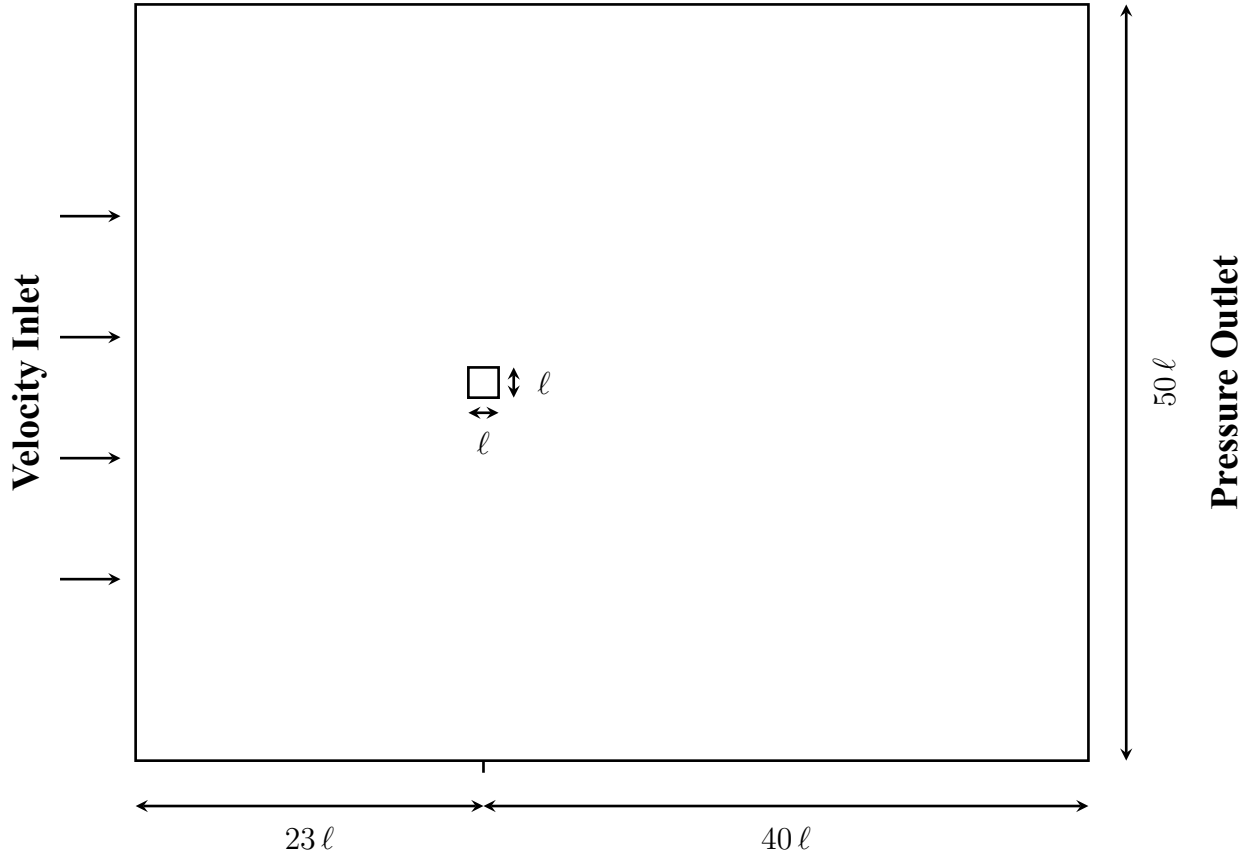


Figure 5: The fluid domain with dimensions. Inspired by comflics (2014)

Given the computational limitations of the computer the simulation was conducted on, an overall length ℓ of 1×10^{-3} meters was chosen, therefore giving each bluff body a characteristic length L of 1×10^{-3} meters.

In order to create the mesh necessary for the simulation, the *All Triangles Method* was utilized. A global unit size of 2.25×10^{-3} meters was applied to the fluid domain to ensure a computationally inexpensive resolution in regions of negligible interest. Conversely, near the edge of the bluff body, a significantly smaller unit size of 2.0×10^{-5} meters was used, constituting an accurate depiction of the interaction between the fluid flow and the bluff body (Ansys Learning, 2023). Furthermore, eight inflation layers were employed in order to accurately capture the gradients associated with boundary layer formation at the edges of the bluff body (Fluid Mechanics 101, 2021). Moreover, a body of influence (BOI) with a sizing of 2.0×10^{-4} meters was used, positioned as shown in 6 below, in order to refine the mesh in the wake region, where the vortex shedding occurs, constituting for a more accurate simulation.

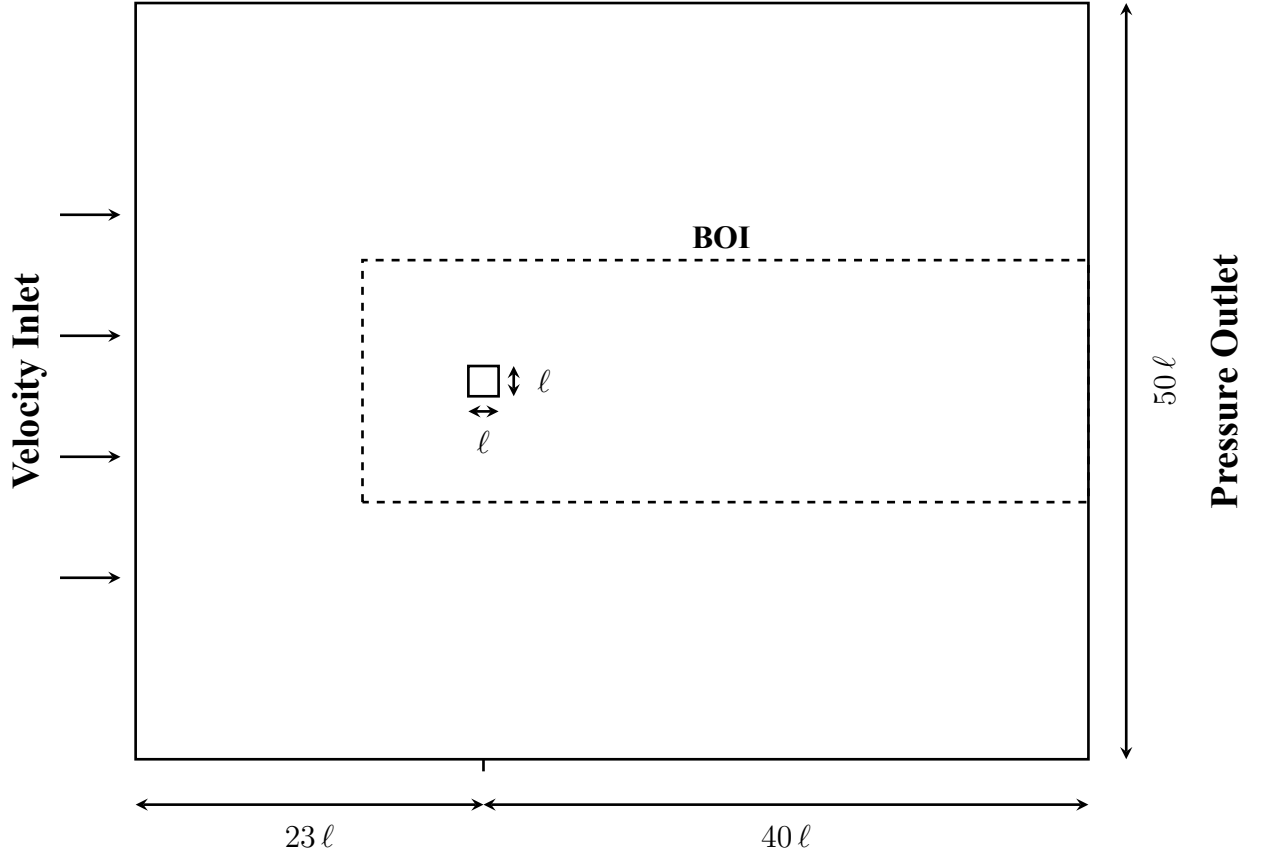


Figure 6: The fluid domain with dimensions. Inspired by comflics (2014)

3.1.2 The OpenFOAM Simulation

The theoretical part of this EE is conducted using the open-source CFD software package OpenFOAM (“OpenFOAM”, 2024). Among the numerous solvers OpenFOAM provides, pimpleFOAM is a transient, pressure-based solver for incompressible, single-phase, also referred to as isothermal, flows. It combines the algorithms used in the pisoFOAM and simpleFOAM solvers, enabling robust handling of transient simulations with larger time steps, allowing for improved computational performance, hence why the solver was chosen. Moreover, its ability to model both laminar and turbulent flow ensures flow conditions are accurately reflected and given that the fluctuations of lift force are sinusoidal, one can verify the flow is laminar. Utilizing reporting functions, one can extract the lift coefficient C_L , which shows the fluctuations in the lift force acting on the bluff body.

3.1.3 Simulation Settings

To adhere to the scope of this essay, the simulation setup is adapted from a case study provided in the Udemy course OpenFOAM for Absolute Beginners by Jayaraj P (2024). The tutorial case *3vortexShedding*, discussed in lecture eight, serves as a structural template and has been modified to align with the specific requirements of this investigation.

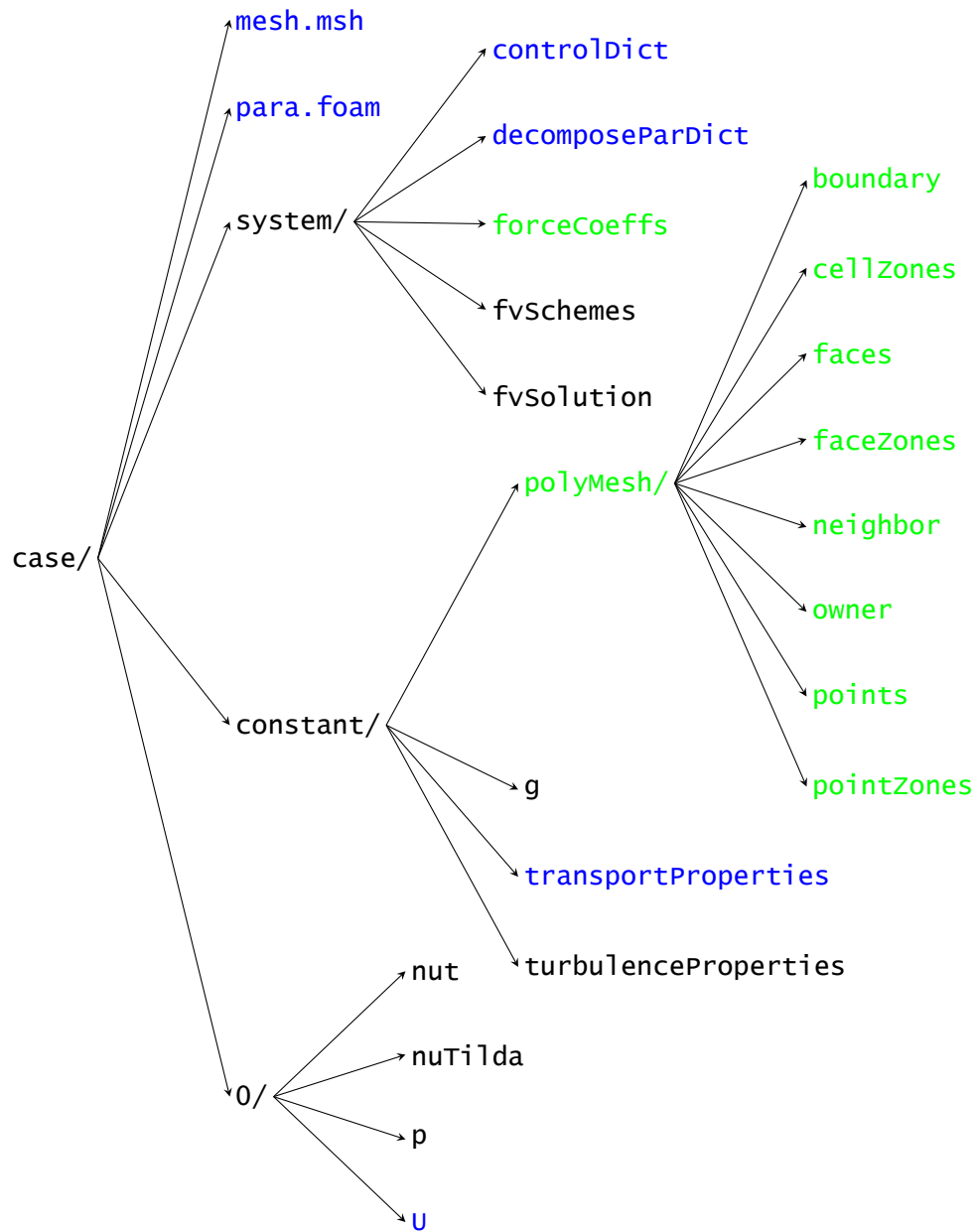


Figure 7: Overview of the simulation directory structure. Modified files are highlighted blue. Created files and folders are highlighted green

| File | Parameter | Original | Modified | Justification |
|---|--------------------|--|--|---|
| mesh.msh, para.foam, polyMesh/ boundary cellZones faces faceZones neighbor owner points pointsZones | — | mesh.msh defines, polyMesh/ contains and para.foam visualizes the mesh of fluid domain of tutorial case | mesh.msh defines, polyMesh/ contains and para.foam visualizes the mesh of fluid domain with dimensions given in Section 3.1.1 | The fluid domain has been adjusted to conform with the computational limits discussed in Section 3.1.1, while achieving the Reynolds number required for this investigation |
| controlDict | deltaT | 0.0002 | 0.00001 | Decreased in order to achieve a greater accuracy (Versteeg & Malalasekera, 2007, p. 289) while ensuring numerical stability (Caminha, 2017). |
| | functions | none | #include "forceCoeffs" | Reporting function defined in forceCoeffs included in order to extract the lift coefficient C_L (Codeynamics, 2024) |
| | adjustTimeStep | yes | no | Removed as the simulation demonstrated stable behavior with the adjusted deltaT (Jayaraj P, 2024) |
| decomposeParDict | numberOfSubdomains | 8 | 6 | The simulations are performed on a system with 6 processing cores (Jayaraj P, 2024) |
| forceCoeffs | — | — | Created a reporting function which outputs the variation of the lift coefficient C_L throughout the simulation | Lift coefficient C_L needed for subsequent calculation of vortex shedding frequency f |

Table 1: Overview of the changes made to the simulation template.

| File | Parameter | Original | Modified | Justification |
|---------------------|--------------------------|-----------------|-----------------|---|
| transportProperties | nu | 1×10^5 | 1×10^6 | The kinematic viscosity of water at 20°C is approximately $1 \times 10^{-6} \text{ m}^2 \text{ s}^{-1}$ (“Water - Dynamic and Kinematic Viscosity at Various Temperatures and Pressures”, n.d.) |
| U | inlet value (x, y, z) | x = 10 | x = 0.1 | Adapted in order to achieve the target Reynolds number of 100 using Equation (2) where $L = 1 \times 10^{-3} \text{ m}$ and $\nu = 1 \times 10^{-6} \text{ m}^2 \text{ s}^{-1}$ |

Table 1 (continued): Overview of the changes made to the simulation template.

3.2 The Practical Investigation

Inspired by the flow tank built by Harvard University’s Science Demonstrations Center (“Vortex Shedding in Water | Harvard Natural Sciences Lecture Demonstrations”, n.d.), the practical part of this EE will be conducted in a self-built flow tank, utilizing a water pump and a separation wall to create flow over a horizontal plate — the water pump moves the water from one side of the separation wall to the other. A second separation wall which fails to reach the bottom of the tank forces the water flowing over the horizontal wall towards the pump. The regulation valve is used to modulate the flow velocity while the sponge diffuser decreases the flow velocity and ensures a uniform distribution of flow. Both a lamp and the addition of potassium permanganate crystals in front of the shape are used in order to better visualize the water flow. The thermal insulation foam ensures watertightness between the aquarium wall and the inside components.

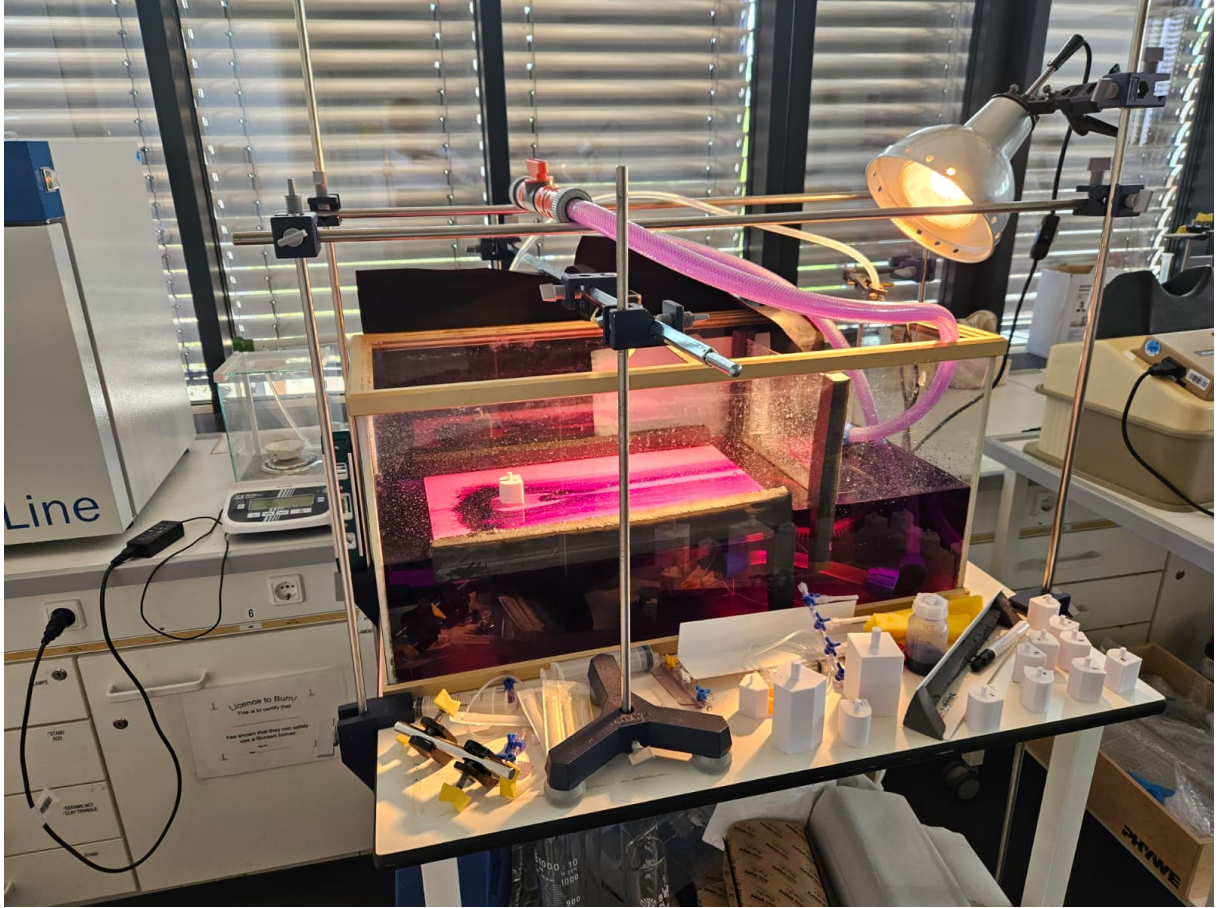


Figure 8: The setup for the practical investigation

The bluff bodies were 3D printed with an overall length ℓ of 0.02 meters — as described in Section 2.5 — giving each shape a characteristic length L of 0.02 meters and a height of 0.04 meters. Reference marks on the horizontal plate ensure the shape is positioned in the same position each trial. A GoPro is mounted parallel to the horizontal plate, ensuring a continuous recording of the entire horizontal plate.

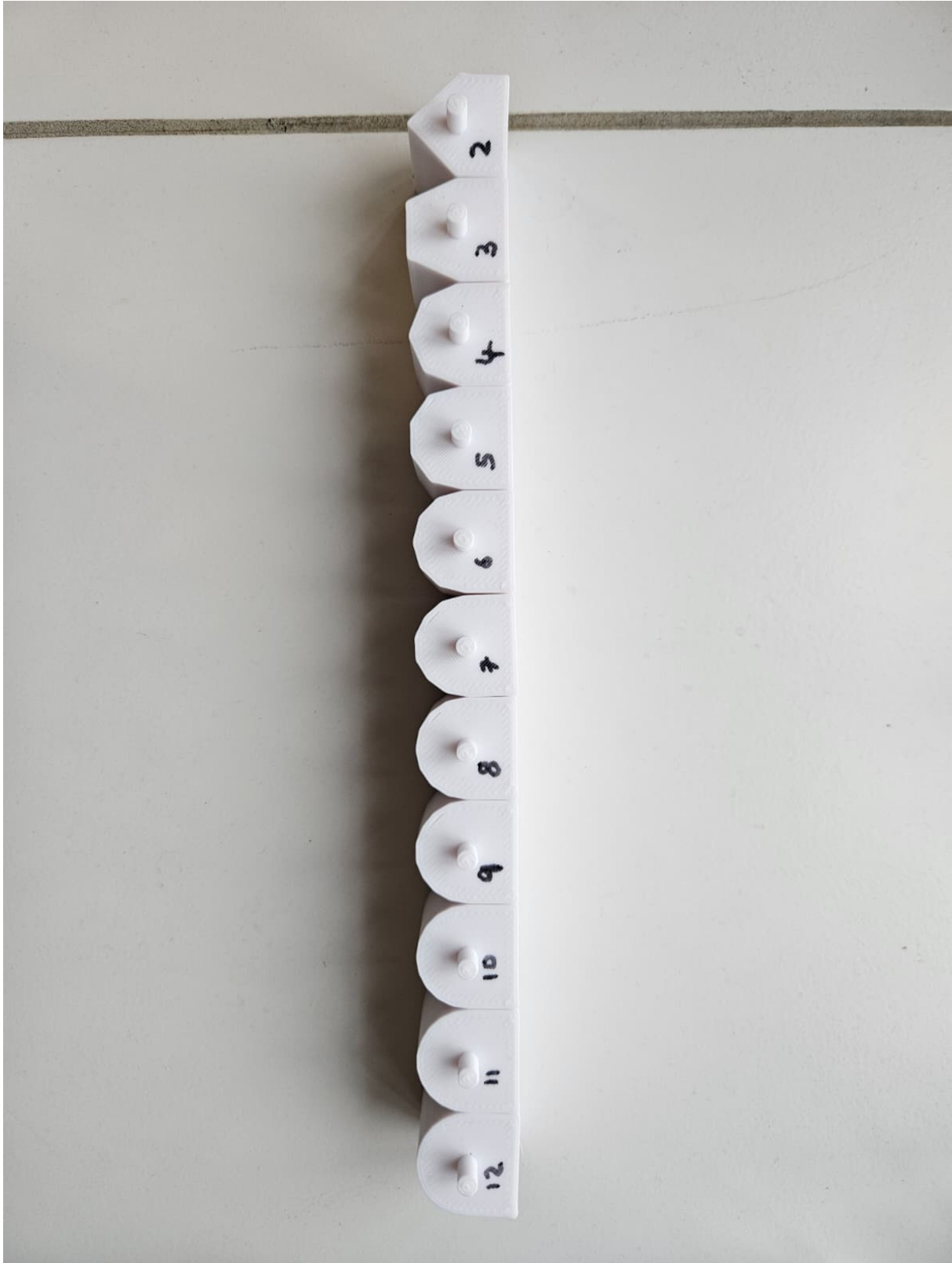


Figure 9: The 3D-printed bluff bodies



Figure 10: A bluff body positioned in the flow tank with potassium permanganate crystals spread in front of it

3.3 Determining the vortex shedding frequency

The inverse relationship given by Equation (1) in section Section 2.1 will be used to determine the vortex shedding frequency. By measuring the time interval between the formation of two consecutive vertices on one side of the bluff body, one can find the time period and therefore the frequency of vortex shedding. To obtain an accurate vortex shedding frequency, the determination of the time period was done multiple times and was only done in the steady-state phase, when the velocity and pressure at any given point in the system remain constant (“Steady State Flow - Fluid Flow Hydraulic and Pneumatic,” n.d.), omitting the initial transient phase, when the velocity and pressure vary over time (“Transient flow”, n.d.). A Fast Fourier Transform approach was not chosen due to the lack of sufficient run time during the trials on either investigation (Shi et al., 2025, pp. 10–11; Xu et al., 2025, p. 12).

4 Variables

| | |
|---|--|
| Independent Variable | Number of faces of the bluff body (ranging from 2 to 12) |
| Dependent Variable | The vortex shedding frequency |
| Constant Variables (Theoretical Investigation) | <ul style="list-style-type: none"> – Characteristic length – Simulation settings – Fluid domain dimensions – Mesh resolution |
| Constant Variables (Practical Investigation) | <ul style="list-style-type: none"> – Characteristic length – Fluid used (water) – Water temperature – Flow velocity – Position of bluff body – Lighting conditions – Camera setup and settings – Measurement duration – Material and surface finish of bluff bodies – Overall length of bluff body |

Table 2: Overview of Variables in the Investigation

5 Equipment

| Theoretical Investigation | Practical Investigation |
|---|--|
| <ul style="list-style-type: none"> – Ansys Work Bench (“Ansys Workbench Simulation Integration Platform”, n.d.) – WSL for Windows (“Windows Subsystem for Linux (WSL)”, n.d.) – OpenFOAM (“OpenFOAM”, 2024) – ParaView (“ParaView - Open-source, multi-platform data analysis and visualization application”, n.d.) – Python (“Welcome to Python.org”, 2025) | <ul style="list-style-type: none"> – Original Prusa MINI 3D Printer with PLA filament (“Original Prusa MINI+ Halbmontiert Original Prusa 3D-Drucker direkt von Josef Prusa”, n.d.) – Slicer for Prusa MINI 3D Printer (“PrusaSlicer Original Prusa 3D-Drucker direkt von Josef Prusa”, n.d.) – FreeCAD (“FreeCAD”, n.d.) – Aquarium of size $1.18\text{ m} \times 0.32\text{ m} \times 0.44\text{ m}$ – 75W Water pump (“Lnicez Schmutzwasser-Tauchpumpe(75 W, Ø19 mm,3.000L/H)”, n.d.) – Waterproof liquid glue – Saw – Piping with diameter 0.017 m – Pipe connectors and corner pieces with diameter 0.017 m – Regulation valve – Thermal insulation foam – Acrylic glass (white coated and clear) – Sponge – Cloth – Knife – Potassium permanganate crystals – Spatula – Permanent Marker |

Table 3: A list of the equipment required for both the theoretical and practical investigation

6 Method

References

- Alammar, A. (n.d.). *Wake of bodies (chapter 1)* [Accessed: 2025-07-14]. https://www.researchgate.net/profile/Ahmed-Alammar/post/How_do_I_ensure_20layers_in_Boundary_layer_during_meshing_FLUENT_OR_CFX/attachment/59d620d379197b807797f458/AS%3A292776961953792%401446814875823/download/wake+of+bodies+6248_chap01.pdf
- Allum, J., & Morris, P. (2023). *Physics* (3rd ed.) [For the IB Diploma Programme]. Hodder Education.
- Ansys Learning. (2023, February 10). *Best practices for mesh generation — lesson 2*. Retrieved June 22, 2025, from <https://www.youtube.com/watch?v=nwrBYdHi64w>
- Ansys workbench | simulation integration platform. (n.d.). Retrieved June 22, 2025, from <https://www.ansys.com/products/ansys-workbench>
- Buresti, G. (1998). Vortex shedding from bluff bodies. *Journal of Wind Engineering and Industrial Aerodynamics*, 74-76, 163–172. [https://doi.org/10.1016/S0167-6105\(98\)00015-5](https://doi.org/10.1016/S0167-6105(98)00015-5)
- Caminha, G. (2017, August 29). *CFL condition: How to choose your timestep size* [SimScale]. Retrieved July 13, 2025, from <https://www.simscale.com/blog/cfl-condition/>
- Choi, C.-K., & Kwon, D. K. (2000). Determination of the strouhal number based on the aerodynamic behavior of rectangular cylinders. *Wind and Structures: An International Journal*, 3(3), 209–220. <https://doi.org/10.12989/was.2000.3.3.209>
- Codeynamics. (2024, January 21). *Prism drag and lift calculation and plotting | cd cl | Open-FOAM CFD | simpleFoam*. Retrieved July 13, 2025, from <https://www.youtube.com/watch?v=hOvGF1DUn8A>
- comflics. (2014, August 27). *OpenFOAM tutorial #4 - laminar vortex shedding*. Retrieved June 22, 2025, from <https://www.youtube.com/watch?v=yIzQXiEdYYo>
- Embry-Riddle Aeronautical University. (n.d.). *Introduction to boundary layers* [Accessed: 2025-05-22]. EaglePubs Open Educational Resources. <https://eaglepubs.erau.edu/introductiontoaerospaceflight/chapter/introduction-to-boundary-layers/>
- Fitzpatrick, R. (2016, March). *Reynolds number* [Accessed: 2025-05-20]. University of Texas at Austin. <https://farside.ph.utexas.edu/teaching/336L/Fluidhtml/node116.html>
- Fluid Mechanics 101. (2021, June 24). *[CFD] inflation layers / prism layers in CFD*. Retrieved June 22, 2025, from <https://www.youtube.com/watch?v=1gSHN99I7L4>
- FreeCAD: Ihr parametrischer 3D-Modellierer. (n.d.). Retrieved July 22, 2025, from <https://www.freecad.org/index.php?lang=de>
- Ghose, T. (2014). *What is fluid dynamics?* [Accessed: 2025-03-12]. LiveScience. <https://www.livescience.com/47446-fluid-dynamics.html>
- Gonçalves, H. C., & Del Rio Vieira, E. (1999). Strouhal number determination for several regular polygon cylinders for reynolds number up to 600 [Accessed: 2025-07-22]. *Proceedings of the 15th Brazilian Congress of Mechanical Engineering (COBEM 1999)*. <https://www.abcm.org.br/anais/cobem/1999/pdf/AACFFE.pdf>
- Govardhan, R., & Ramesh, O. (2005). A stroll down kármán street. *Resonance*, 10, 25–37. <https://doi.org/10.1007/BF02866744>
- Green, S. I. (Ed.). (1995). *Fluid vortices* (Vol. 30) [Softcover reprint of the hardcover 1st edition, originally published in 1995]. Kluwer Academic Publishers. <https://doi.org/10.1007/978-94-011-0249-0>
- Holton, J. R. (2003). Vorticity. In J. R. Holton (Ed.), *Encyclopedia of atmospheric sciences* (pp. 2500–2504). Academic Press. <https://doi.org/10.1016/B0-12-227090-8/00449-8>

- Ib physics guide 2025 [Accessed: 2025-02-27]. (2023). *International Baccalaureate Organization*. <https://peda.net/kuopio/lukiot/lyseonlukio/ib/syllabukset/group-4-sciences/physics-2025.pdf>: file/download/c56a8c8592e847bbb555540b087b0990d1ade5b0/Physics%2C%202025.pdf
- Ilieva, G. (2017). On turbulence and its effects on aerodynamics of flow through turbine stages. In *Turbomachinery*. InTech. <https://doi.org/10.5772/intechopen.68205>
- Jayaraj P, H. (2024). *Lecture: Introduction to vortex shedding simulation using openfoam* [From the course "OpenFOAM for Absolute Beginners", Codeynamics on Udemy]. Udemy. <https://www.udemy.com/course/openfoam-for-absolute-beginners/learn/lecture/44356412>
- Jeff Defoe. (2020, May 26). *Bluff body aerodynamics, lecture 2 part 5*. Retrieved June 22, 2025, from <https://www.youtube.com/watch?v=9g62QkNFtIE>
- Jurado, J. Á., Sánchez, R., Hernández, S., Nieto, F., & Kusano, I. (2012). A review of cases of vortex shedding excitation in bridges: Sectional models testing [Accessed: 2025-05-04]. *Proceedings of the Seventh International Colloquium on Bluff Body Aerodynamics and Applications (BBAA7)*. <https://iawe.org/Proceedings/BBAA7/J.Jurado.pdf>
- Learn Engineering. (2022, August). *What is boundary layer in fluid mechanics* [Accessed: 2025-04-16]. <https://www.youtube.com/watch?v=ahohd8ceGR4>
- Lnicez *schmutzwasser-tauchpumpe(75 w, ø19 mm,3.000l/h)*. (n.d.). Retrieved July 22, 2025, from https://www.amazon.de/dp/B0987LCYMK?ref=ppx_yo2ov_dt_b_fed_asin_title&th=1
- Mohn, E. (2024). *Non-newtonian fluid* [Accessed: 2025-04-30]. EBSCO Information Services. <https://www.ebsco.com/research-starters/science/non-newtonian-fluid>
- NASA Glenn Research Center. (2021). *Reynolds number* [Accessed: 2025-05-13]. NASA. <https://www.grc.nasa.gov/www/k-12/airplane/reynolds.html>
- National Research Council. (1997). *Twenty-first symposium on naval hydrodynamics* [Symposium held in Trondheim, Norway, June 24–28, 1996. Accessed: 2025-06-22]. National Academies Press. <https://doi.org/10.17226/5870>
- Nitsche, M. (2006). Vortex dynamics. In J.-P. Francoise, G. L. Naber, & S. T. Tsou (Eds.), *Encyclopedia of mathematical physics* (pp. 390–399). Academic Press. <https://doi.org/10.1016/B0-12-512666-2/00254-6>
- OpenFOAM*. (2024, December 24). Retrieved June 22, 2025, from <https://www.openfoam.com/>
- Oran, E. S., & Boris, J. P. (2002). Fluid dynamics. In R. A. Meyers (Ed.), *Encyclopedia of physical science and technology* (3rd ed., pp. 31–43). Academic Press. <https://doi.org/10.1016/B0-12-227410-5/00248-9>
- Original Prusa MINI+ Halbmontiert | Original Prusa 3D-Drucker direkt von Josef Prusa* [Prusa3D by Josef Prusa]. (n.d.). Retrieved July 22, 2025, from <https://www.prusa3d.com/de/produkt/original-prusa-mini-halbmontiert-4/>
- ParaView - open-source, multi-platform data analysis and visualization application*. (n.d.). Retrieved July 21, 2025, from <https://www.paraview.org/>
- PrusaSlicer | Original Prusa 3D-Drucker direkt von Josef Prusa* [Prusa3D by Josef Prusa]. (n.d.). Retrieved July 22, 2025, from https://www.prusa3d.com/de/page/prusaslicer_424/
- The relationship between reynolds number and kinematic viscosity*. (n.d.). Retrieved July 14, 2025, from <https://resources.system-analysis.cadence.com/blog/msa2022-the-relationship-between-reynolds-number-and-kinematic-viscosity>
- Rocchi, D., & Zasso, A. (2002). Vortex shedding from a circular cylinder in a smooth and wired configuration: Comparison between 3d les simulation and experimental analysis. *Jour-*

- nal of Wind Engineering and Industrial Aerodynamics*, 90(4–5), 475–489. [https://doi.org/10.1016/S0167-6105\(01\)00203-3](https://doi.org/10.1016/S0167-6105(01)00203-3)
- Saldana, M., Gallegos, S., Gálvez, E., Castillo, J., Salinas-Rodríguez, E., Cerecedo-Sáenz, E., Hernández-Ávila, J., Navarra, A., & Toro, N. (2024). The reynolds number: A journey from its origin to modern applications. *Fluids*, 9(12), 299. <https://doi.org/10.3390/fluids9120299>
- Shen, H.-M., Fu, X., Chen, J.-D., & Ye, P. (2010). Development of a vortex flowmeter with good performance at low-flowrate [Accessed: 2025-06-22]. *Proceedings of the 15th International Flow Measurement Conference (FLOMEKO)*, 1–6. <https://www.imeko.org/publications/tc9-2010/IMEKO-TC9-2010-017.pdf>
- Shi, F., Ou, C., Xin, J., Li, W., Jin, Q., Tian, Y., & Zhang, W. (2025). Numerical study on hydrodynamic performance and vortex dynamics of multiple cylinders under forced vibration at low reynolds number. *Journal of Marine Science and Engineering*, 13(2), 214. <https://doi.org/10.3390/jmse13020214>
- Song, D., Kim, W., Kwon, O.-K., & Choi, H. (2022). *Vertical and torsional vibrations before the collapse of the tacoma narrows bridge in 1940*. <https://doi.org/10.1017/jfm.2022.748>
- Steady state flow - fluid flow hydraulic and pneumatic*, (n.d.). Retrieved June 23, 2025, from https://www.engineersedge.com/fluid_flow/steady_state_flow.htm
- Transient flow* [Fluid mechanics ltd]. (n.d.). Retrieved June 23, 2025, from <https://www.fluidmechanics.co.uk/hydraulic-calculations/transient-flow/>
- TutorialsPoint. (2018, January 23). *Boundary layer theory - introduction*. Retrieved June 22, 2025, from <https://www.youtube.com/watch?v=54zf68IoPWU>
- Versteeg, H. K., & Malalasekera, W. (2007). *An introduction to computational fluid dynamics: The finite volume method* (2nd ed.). Pearson Education.
- Vortex shedding in water | harvard natural sciences lecture demonstrations*. (n.d.). Retrieved June 23, 2025, from <https://sciencedemonstrations.fas.harvard.edu/presentations/vortex-shedding>
- Water - dynamic and kinematic viscosity at various temperatures and pressures*. (n.d.). Retrieved July 13, 2025, from https://www.engineeringtoolbox.com/water-dynamic-kinematic-viscosity-d_596.html
- Welcome to python.org* [Python.org]. (2025, July 16). Retrieved July 21, 2025, from <https://www.python.org/>
- Windows subsystem for linux (WSL)* [Ubuntu]. (n.d.). Retrieved July 21, 2025, from <https://ubuntu.com/desktop/wsl>
- Xu, G., Yu, W., Sciacchitano, A., & Simao Ferreira, C. (2025). An experimental study of the unsteady aerodynamics of a static DU91-w2-150 airfoil at large angles of attack. *Wind Energy*, 28(3), e2974. <https://doi.org/10.1002/we.2974>